The Astrophysical Journal Letters, 728:L31 (5pp), 2011 February 20 doi:10.1088/2041-8205/728/2/L31

SUCCESSIVE MERGER OF MULTIPLE MASSIVE BLACK HOLES IN A PRIMORDIAL GALAXY

A. Tanikawa and M. Umemura
Center for Computational Sciences, University of Tsukuba, 1-1-1 Ten-nodai, Tsukuba, Ibaraki 305-8577, Japan
Received 2010 July 12; accepted 2011 January 11; published 2011 January 27

ABSTRACT

Using highly accurate *N*-body simulations, we explore the evolution of multiple massive black holes (hereafter MBHs) in a primordial galaxy that is composed of stars and MBHs. The evolution is pursed with a fourth-order Hermite scheme, where not only three-body interaction of MBHs but also dynamical friction by stars are incorporated. Initially, 10 MBHs with equal masses of $10^7\,M_\odot$ are set in a host galaxy with $10^{11}\,M_\odot$. It is found that 4–6 MBHs merge successively within 1 Gyr, emitting gravitational wave radiation. The key process for the successive merger of MBHs is the dynamical friction by field stars, which enhances three-body interactions of MBHs when they enter the central regions of the galaxy. The heaviest MBH always composes a close binary at the galactic center, which shrinks owing to the angular momentum transfer by the third MBH and eventually merges. The angular momentum transfer by the third MBH is due to the sling-shot mechanism. We find that the secular Kozai mechanism does not work for a binary to merge if we include the relativistic pericenter shift. The simulations show that a multiple MBH system can produce a heavier MBH at the galactic center purely through *N*-body process. This merger path can be of great significance for the growth of MBHs in a primordial galaxy. The merger of multiple MBHs may be a potential source of gravitational waves for the *Laser Interferometer Space Antenna* and pulsar timing.

Key words: black hole physics – galaxies: nuclei – methods: numerical

1. INTRODUCTION

Massive black holes (hereafter MBHs) with 10^6–$10^9\,M_\odot$ are found to reside in the central regions of galaxies. They are believed to coevolve with their host galaxies, since the masses of MBHs correlate with the mass and velocity dispersion of the spheroidal components of the host galaxies (Kormendy & Richstone 1995; Magorrian et al. 1998; Ferrarese & Merritt 2000; Tremaine et al. 2002; Marconi & Hunt 2003). Such MBHs seem to acquire most of their mass through gas accretion in the final evolutionary stage (Soltan 1982; Yu & Tremaine 2002). But, the growth from order-of-magnitude smaller BHs is still unresolved.

In the last decade, many quasars at redshift $z \sim 6$ have been observed (e.g., Fan et al. 2001). This suggests that MBHs with $10^9\,M_\odot$ have formed when the age of the universe was only 1 Gyr. If seed BHs are the remnants of first stars with $\sim 100\,M_\odot$ (Abel et al. 2000; Nakamura & Umemura 2001; Bromm et al. 2002; Yoshida et al. 2006), the seed BHs cannot grow to $10^9\,M_\odot$ with a continuous Eddington accretion rate over 1 Gyr. One solution is growth by super-Eddington accretion (e.g., Abramowicz et al. 1988; Ohsuga et al. 2005). However, gas accretion onto the seeds should be intermittent, and on average could be lower than the Eddington accretion (Milosavljevic et al. 2009a, 2009b).

Hence, it is worth considering the possibility of BH mergers for the growth of MBHs. In the cold dark matter cosmology, a massive galaxy forms through the multiple merger of subgalaxies. If subgalaxies possess MBHs, a massive galaxy should contain multiple MBHs shortly after the merger. On the other hand, besides some candidates of binary MBHs (e.g., Sudou et al. 2003; Boroson & Lauer 2009; Dotti et al. 2009), there is little evidence for multiple MBHs in a massive galaxy. Thus, multiple MBHs possibly merge into a heavier BH. But, the merger path of multiple MBHs in a massive galaxy has not been hitherto resolved.

In this Letter, we explore the evolution of the system of multiple MBHs in a massive galaxy. Previous studies found that if two MBHs are in one galaxy, it is difficult for them to merge within a Hubble time due to loss-cone depletion (Begelman et al. 1980; Makino & Funato 2004). If three MBHs are in one galaxy, two of them merge or result in a binary, and the other is ejected from the galaxy (Iwasawa et al. 2006). Here, we consider a two-component system that consists of MBHs and stars, where not only three-body interaction of MBHs but also dynamical friction by stars are incorporated. The Letter is organized as follows. In Section 2, we describe our simulation method to follow the evolution of the multiple MBHs. In Section 3, simulation results are presented. In Section 4, we discuss the validity of our model. In Section 5, we summarize this Letter.

2. METHOD

2.1. Setup

We treat MBHs and stars as an *N*-body system. An individual MBH corresponds to one massive particle, and field stars composing a host galaxy are approximated as super particles, a fraction of which may be interpreted as dark matter.

The field stars are distributed according to the Hernquist model (Hernquist 1990), whose radial mass density distribution, $\rho(r)$, is given by

$$\rho(r) = \frac{M}{6\pi r_{\rm v}^3} \frac{1}{(r/r_{\rm v})\,[(r/r_{\rm v}) + 1/3]^3}, \quad (1)$$

where M and $r_{\rm v}$ are the total mass and virial radius of the galaxy, respectively. The virial radius is given by $r_{\rm v} = GM/4|E|$, where G is the gravitational constant and E is the total energy of the galaxy. The number of the field stars is $N = 512K (1K = 1024)$.

Here, 10 MBHs with equal mass of $10^7\,M_\odot$ are set in a galaxy with $10^{11}\,M_\odot$. This means that the total mass of the MBHs is 0.1% of the galaxy mass and the mass ratio of each MBH to each field star is about 50. We perform five simulations with different phase-space distributions of the MBHs at the initial

Table 1
Summary for Our Simulation Results

Model Name	$r_{\rm MBH}/r_{\rm v}$	Rand No.	$10^4 m_{\rm B,max}$	$10^4 m_{\rm B,sec}$
A_1	1/3	R1	4	3 (ejected)
A_2	1/3	R2	4	1
A_3	1/3	R3	6	1
B	2/3	R1	5	1
C	1	R1	5	1

time in order to see the dependence on the stellar mass density around the MBHs. The MBHs are distributed initially within one-third, two-thirds, and one virial radius of the galaxy in models A, B, and C, respectively. Furthermore, in model A, the positions of MBHs are changed according to three different sets of random numbers, which are labeled by models A_1, A_2, and A_3, respectively. These models are summarized in Table 1.

In the present simulations, we adopt the standard N-body units, $G = M = r_{\rm v} = 1$. In such units, the time unit of simulation, $t_{\rm nu}$, is comparable to the dynamical time, $t_{\rm nu} \sim t_{\rm dy}$. The light speed is $c = 600$ in these units, which means that the three-dimensional velocity dispersion of field stars is 300 km $\rm s^{-1}$ at the galaxy center.

If we convert the N-body units to physical units, the virial radius, the dynamical timescale within the virial radius, $t_{\rm dy}$, and the average mass density of the galaxy within the virial radius, $\rho_{\rm v}$, are, respectively, given by

$$r_{\rm v} \sim 2 \left(\frac{M}{10^{11} M_\odot} \right) ({\rm kpc}), \tag{2}$$

$$t_{\rm dy} \sim 6 \left(\frac{M}{10^{11} M_\odot} \right) ({\rm Myr}), \tag{3}$$

$$\rho_{\rm v} \sim 1 \left(\frac{M}{10^{11} M_\odot} \right)^{-3} (M_\odot\,{\rm pc}^{-3}). \tag{4}$$

According to this scaling, the present results can be applicable for the different mass system, which is discussed later.

2.2. Merger Condition

We assume that two MBHs merge through gravitational wave radiation when the separation between two MBHs is less than 10 times the sum of their Schwarzschild radii:

$$|\mathbf{r}_{{\rm B},i} - \mathbf{r}_{{\rm B},j}| < 10\,(r_{{\rm sch},i} + r_{{\rm sch},j}), \tag{5}$$

where $\mathbf{r}_{{\rm B},i}$ and $r_{{\rm sch},i}$ are the position and Schwarzschild radius of the ith MBH. The Schwarzschild radius of the ith MBH is $r_{{\rm sch},i} = 2Gm_{{\rm B},i}/c^2$ for the MBH mass $m_{{\rm B},i}$.

2.3. Equation of Motion

The equations of motion for field stars and MBHs are, respectively, given by

$$\frac{d^2\mathbf{r}_{{\rm f},i}}{dt^2} = \sum_{j\neq i}^{N_{\rm f}} \mathbf{a}_{{\rm ff},ij} + \sum_{j}^{N_{\rm B}} \mathbf{a}_{{\rm fB},ij} \tag{6}$$

$$\frac{d^2\mathbf{r}_{{\rm B},i}}{dt^2} = \sum_{j}^{N_{\rm f}} \mathbf{a}_{{\rm Bf},ij} + \sum_{j\neq i}^{N_{\rm B}} \mathbf{a}_{{\rm BB},ij}, \tag{7}$$

where $\mathbf{r}_{{\rm f},i}$ and $\mathbf{r}_{{\rm B},i}$ are the positions of the ith field star and MBH, $N_{\rm f}$ and $N_{\rm B}$ are the numbers of field stars and MBHs, $\mathbf{a}_{{\rm ff},ij}$ and $\mathbf{a}_{{\rm fB},ij}$ are the accelerations of the jth field star and MBH on the ith field star, and $\mathbf{a}_{{\rm Bf},ij}$ and $\mathbf{a}_{{\rm BB},ij}$ are the accelerations of the jth field star and MBH on the ith MBH, respectively. Excepting the MBH–MBH interaction, the accelerations are given by Newtonian gravity:

$$\mathbf{a}_{{\rm ff},ij} = -\,Gm_{{\rm f},j} \frac{\mathbf{r}_{{\rm f},i} - \mathbf{r}_{{\rm f},j}}{(|\mathbf{r}_{{\rm f},i} - \mathbf{r}_{{\rm f},j}|^2 + \epsilon^2)^{3/2}} \tag{8}$$

$$\mathbf{a}_{{\rm fB},ij} = -\,Gm_{{\rm B},j} \frac{\mathbf{r}_{{\rm f},i} - \mathbf{r}_{{\rm B},j}}{|\mathbf{r}_{{\rm f},i} - \mathbf{r}_{{\rm B},j}|^3} \tag{9}$$

$$\mathbf{a}_{{\rm Bf},ij} = -\,Gm_{{\rm f},j} \frac{\mathbf{r}_{{\rm B},i} - \mathbf{r}_{{\rm f},j}}{|\mathbf{r}_{{\rm B},i} - \mathbf{r}_{{\rm f},j}|^3}, \tag{10}$$

where $m_{{\rm f},j}$ and $m_{{\rm B},j}$ are, respectively, the masses of the jth field star and MBH, and the softening parameter ($\epsilon = 10^{-3}$) is introduced only in star–star interactions.

The acceleration between two MBHs contains Newtonian gravity and post-Newtonian corrections, such as

$$\mathbf{a}_{{\rm BB},ij} = -Gm_{{\rm B},j} \frac{\mathbf{r}_{{\rm B},i} - \mathbf{r}_{{\rm B},j}}{|\mathbf{r}_{{\rm B},i} - \mathbf{r}_{{\rm B},j}|^3} + \mathbf{a}_{{\rm PN},ij}. \tag{11}$$

For the second term ($\mathbf{a}_{{\rm PN},ij}$), the pericenter shift (1PN and 2PN terms) as well as the gravitational radiation emission (2.5PN term) is considered (Damour & Dervelle 1981; Soffel 1989; Kupi et al. 2006). We adopt Equations (1)–(4) in Kupi et al. (2006) for the second term.

If the semimajor axis is less than $a_{\rm crit} = 5 \times 10^{-5}$, the motion of the binary is transformed to the motion of the center of mass and the relative motion. We ignore tidal forces by distant field stars on the binary. Then, the acceleration by a distant field star k to the center of mass ($a_{{\rm cm},k}$) and the relative motion ($a_{{\rm rel},k}$) is approximated as

$$\mathbf{a}_{{\rm cm},k} \approx -\,Gm_{{\rm f},k} \frac{\mathbf{r}_{\rm cm} - \mathbf{r}_{{\rm f},k}}{|\mathbf{r}_{\rm cm} - \mathbf{r}_{{\rm f},k}|^3}, \tag{12}$$

$$\mathbf{a}_{{\rm rel},k} \approx 0, \tag{13}$$

where $\mathbf{r}_{\rm cm}$ is the position of the center of mass of the MBH binary. Distant field stars are defined as

$$|\mathbf{r}_{\rm cm} - \mathbf{r}_{{\rm f},k}| > Ca_{\rm crit}, \tag{14}$$

where $C = 200$.

2.4. Numerical Scheme

We use a fourth-order Hermite scheme with individual time step (Makino & Aarseth 1992) and block time step (McMillan 1986) for field stars, MBHs, and the relative motion in binary MBHs. As for the motion of the center of mass of MBH binaries, a fourth-order Hermite Ahmad–Cohen scheme (Makino & Aarseth 1992) is employed. In a Hermite Ahmad–Cohen scheme, the acceleration due to single MBHs or stars near a binary MBH and those due to distant stars are calculated on separate time steps, which we call "neighbor step" and "distant step," respectively.

The time step except the neighbor step is determined as

$$\Delta t = \sqrt{\eta f(\mathbf{a})}, \tag{15}$$

where η is the accuracy parameter and $\mathbf{a}$ is the acceleration of a field star, a single MBH, or the relative motion of a binary MBH. The function f in Equation (15) is given by

$$f(\mathbf{x}) = \frac{|\mathbf{x}||\mathbf{x}^{(3)}| + |\mathbf{x}^{(2)}|^2}{|\mathbf{x}^{(1)}||\mathbf{x}^{(4)}| + |\mathbf{x}^{(3)}|^2}. \tag{16}$$

The accuracy parameter is set to be $\eta = 0.01$ for time step of field stars, $\eta = 0.0025$ for time step of single MBHs and distant step of the center of mass of binary MBHs, and $\eta = 0.000625$ for the relative motion in binary MBHs. The time step for the center of mass of a binary MBH is determined as

$$\Delta t = \sqrt{\min\left[\eta_1 f(\mathbf{a}), \eta_2 f(\mathbf{a}_{\rm PN})\right]}, \tag{17}$$

where $\eta_1 = 0.0025$ and $\eta_2 = 0.000625$ are the accuracy parameters, and $a_{\rm PN}$ is the acceleration due to post-Newtonian corrections for the center of mass of a binary MBH. The relative error in our simulations is less than 0.1% regarding the total energy.

We perform simulations with 64 nodes of the FIRST simulator in University of Tsukuba (Umemura et al. 2008). At each node, the FIRST simulator is equipped with one Blade-GRAPE board, which is the accelerator of the gravity calculations for collisional N-body problem. The gravity by field stars for a given field star and MBH is calculated in parallel.

3. RESULTS

3.1. *Merger of Multiple MBHs*

We calculate a system of 10 MBHs in one galaxy during about 140 N-body time units, which corresponds to about 800 Myr in physical units. We find that several MBHs merge into one for all simulations. We summarize MBH masses at the final time of simulations in Table 1. The heaviest MBH has $m_{\rm B,max} = (4\text{–}6) \times 10^{-4}$, while the second heaviest MBH has $m_{\rm B,sec} = 1 \times 10^{-4}$, except for model $\rm A_1$. The growth of such a dominant MBH is weakly dependent on the initial stellar mass density around MBHs.

We see the process in which only one MBH grows in each simulation, using the result of model $\rm A_3$ as a typical case. As shown in the top panel of Figure 1, only one MBH grows and other MBHs do not grow. The second and third panels of Figure 1 show that MBHs compose a binary with a semimajor axis less than 10^{-4} for a longer time than the dynamical time ($t_{\rm dy} \sim 1$). When a binary merges to form a heavier MBH, a lighter component is often exchanged by a third MBH. Thereafter, a binary MBH forms again, containing the heaviest MBH (see the fourth panel of Figure 1). This is because a heavier MBH is easier to be retained in a binary MBH through an interaction between the binary MBH and single MBH. Consequently, only one heavy MBH grows in a galaxy.

The reason why no other MBHs merge is understood as follows. When a binary MBH forms in a galaxy, the binary prevents the formation of another binary MBH, because the preformed binary MBH gives other MBHs kick velocities. Since MBHs cannot merge without forming a binary MBH, no other MBHs can merge.

In model $\rm A_1$, the first binary forms just temporarily. It is ejected with a speed of more than 1000 km s^{-1} due to the back-reaction of sling-shot mechanism, when the binary with masses of 2×10^{-4} and 1×10^{-4} merges through the sling-shot mechanism of an interaction MBH. After the ejection, the second binary forms and merges to produce the MBH with mass of 4×10^{-4} through the same process as described above. In our simulations, the ejection by the sling-shot interaction is observed only once. In all the simulations, the merger of binary MBHs occurs 21 times in total. Hence, the ejection of the heaviest MBH due to the sling-shot seems rare.

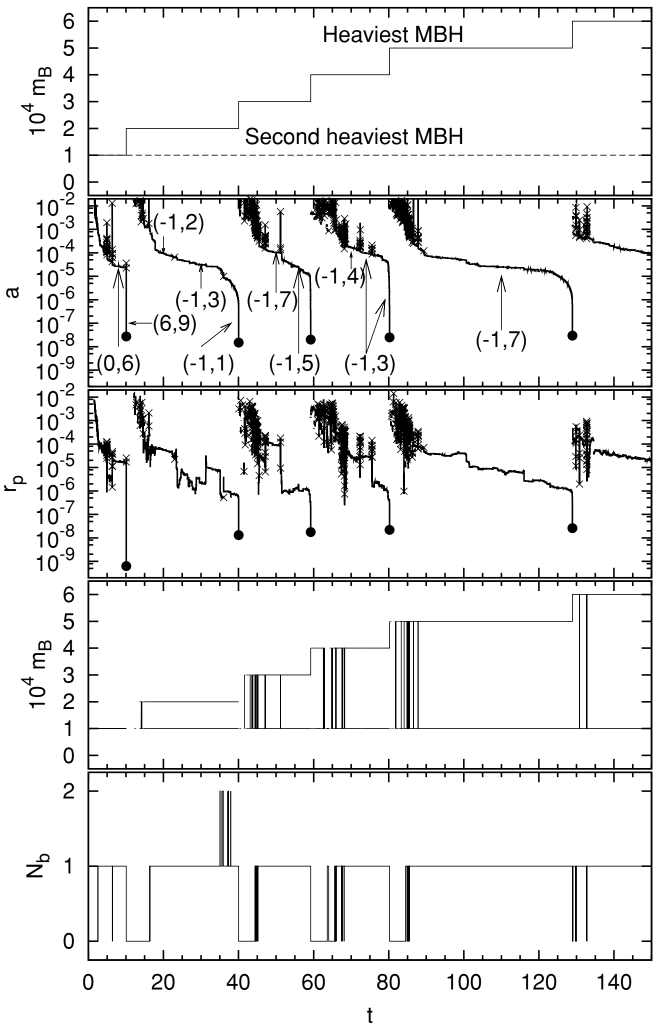

Figure 1. Time evolution of MBHs in model $\rm A_3$. From top to bottom, the panels show the mass of the heaviest MBH and second heaviest at each time, the semimajor axis, the distance at the pericenter, the masses of two MBHs when a binary forms, and the number of binary MBHs. As for the number of binary MBHs, we only count binary MBHs whose semimajor axes are less than 10^{-3}. Pairs of integers in the second panel show the labels of MBHs composing the binary MBHs, where the heaviest MBH is labeled with "-1." We attached labels only to binary MBHs which are long-lived, or merge eventually. In the second top and middle panels, filled circles indicate the moments when MBHs merge and crosses denote those when binary components are exchanged.

3.2. *Merger Mechanism of a Binary MBH*

For the mergers of the MBHs, the dynamical friction plays a key role. In Figure 2, the time variation of the distance of the third nearest MBH from the galactic center is shown, where the result in the N-body simulation and that in a fixed potential of the Hernquist model are compared. In the fixed potential, no dynamical friction is exerted. As seen in this figure, the dynamical friction by field stars in the N-body simulation allows the MBHs to gather near the galaxy center. Thus, two MBHs can compose a binary MBH, and subsequently another MBH can intrude on the binary MBH. In contrast, in a fixed potential,

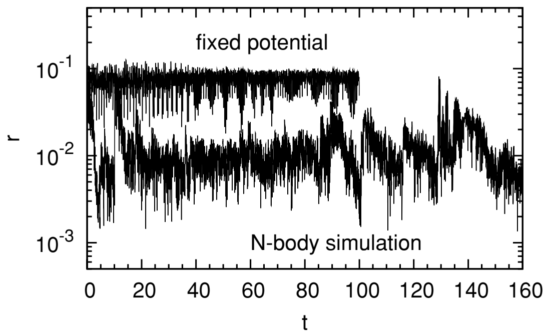

Figure 2. Time variation of the distance of the third nearest MBH from the galactic center. The result in model A_3 and that in a fixed potential are compared.

even a binary MBH cannot be formed, since they cannot gather at around the galaxy center.

Here, we see the details of the merger mechanism of binary MBHs. In Figure 3, the processes of the second merger of MBHs are shown in models A_2 and A_3. The second merger in model A_2 is the simplest case. The binary MBH and a single MBH approach each other and strongly interact. Consequently, the distance of the binary MBH at the pericenter shrinks, followed by emitting gravitational wave radiation and merger. In practice, another single MBH often intrudes into the binary MBH whose orbit is being decayed due to energy loss through gravitational wave radiation, and subsequently the semimajor axis and eccentricity of the binary MBH are changed, as seen in the middle and bottom panels of Figure 3. However, the crucial impact is brought by one strong interaction. In our five simulations, the simultaneous interaction of multiple MBHs that triggers the merger of an MBH binary does not occur.

Also, we have not observed the secular angular momentum loss of a binary MBH through the Kozai mechanism (Kozai 1962). The Kozai mechanism can occur only if the internal orbit of the binary MBH is closed in every binary period. However, the internal orbit is not closed due to the relativistic pericenter shift (1PN and 2PN; Blaes et al. 2002; Berentzen et al. 2009). Actually, we have found that the Kozai mechanism works for a binary to merge only if we do not include the 1PN and 2PN terms. The suppression of the Kozai mechanism is also demonstrated in the case of stellar-sized BHs (Miller & Hamilton 2002) and in the planetary orbits (Fabrycky & Tremaine 2007).

4. DISCUSSION

The present simulations have the scalings shown in Equations (2)–(4). Thus, the present results are applicable for the different mass scales of a host galaxy and MBHs, if the density of the host galaxy satisfies the scaling. For instance, if the collapse redshift of a host galaxy is shifted from $z = 6$ to $z = 10$, the virial density of the host galaxy is expected to be increased by a factor of 3.9. Hence, the same merger processes of MBHs are expected for a host galaxy with $2.6 \times 10^{10} M_{\odot}$ and MBHs with equal mass of $2.6 \times 10^{6} M_{\odot}$.

In the present model, the host galaxy is assumed to have a spherical Hernquist profile. MBHs ejected from the center on a nearly radial orbit with speed below that of the escape speed repeatedly return to the center in our spherical model. However, these MBHs do not contribute much to the merger of binary MBHs. We have found that there is no time for such MBHs to interact with binary MBHs, since they pass the center with high speed. MBHs that gather toward the galactic center by

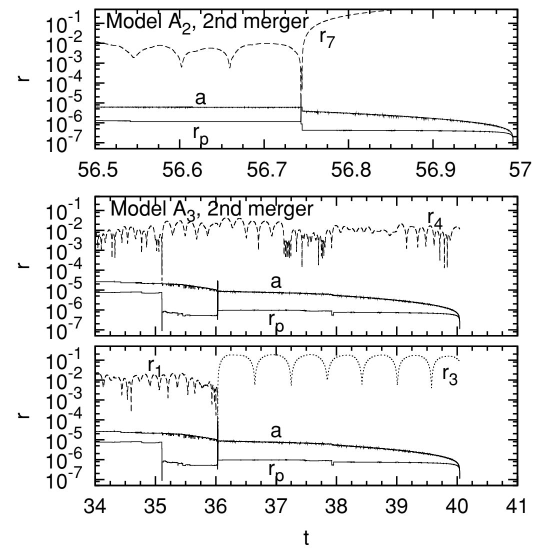

Figure 3. Time variation of the semimajor axes, a, and the distance at the pericenter of binary MBHs, r_p, just before the second mergers in models A_2 (top) and A_3 (middle and bottom). Also, the separation between the center of mass of the binary MBHs and single MBHs which interact strongly with the binary MBHs is shown by dashed and dotted curves (r_7, r_4, r_1, and r_3), where the numbers attached to r are the labels of MBHs. The bottom panel demonstrates the exchange interaction where one binary component is replaced by another single MBH.

dynamical friction more effectively contribute to the merger of a binary MBH.

We have ignored the recoil by a gravitational wave. Unless BH spins are aligned, the recoil velocity can reach up to 4000 km s^{-1} (Campanelli et al. 2007; Lousto et al. 2010). Such a large recoil velocity can eject the merger remnant from the galaxy. However, if their spins are aligned before their merger due to relativistic spin precession (Kesden et al. 2010), then the recoil velocity decreases to a few 100 km s^{-1}. If the recoil velocity is a few 100 km s^{-1}, the merger remnant is possibly confined in a host galaxy with the velocity dispersion of 300 km s^{-1}. Then, the recoil may not affect the results dramatically. Nonetheless, it seems worth carefully exploring the effects of recoil, which will be considered in the future analysis.

We have assumed that a binary MBH immediately merges at the moment when their separation becomes smaller than 10 times the sum of their Schwarzschild radii. In practice, binary MBHs take a bit more time to merge. But, the timescale is too short for the merger to be disturbed by the intrusion of another MBH. The merging timescale of a binary MBH is $\sim 10^{-12}$ in N-body units, while it interacts with an MBH once a dynamical time of the galaxy, ~ 1 in N-body units. Actually, as seen in Figure 3, no MBHs approach the binary MBHs after the semimajor axis becomes about 10^{-7} length unit.

5. SUMMARY

We have performed highly accurate N-body simulations to explore the evolution of multiple MBHs in one galaxy. Here, 10 MBHs with equal mass of $10^{7} M_{\odot}$ are set in a galaxy with $10^{11} M_{\odot}$. As a result, it is found that 4–6 MBHs successively merge, resulting in a single heavier MBH within 1 Gyr. The growth timescale is shorter than a Hubble time at redshift $z \sim 6$. After 4–6 MBHs merge, the other MBHs in the galaxy have the same masses as those at the initial time.

The key physics for the successive merger is the dynamical friction that allows the formation of binary MBHs and frequent interactions of single MBHs with the binary MBHs at the galactic center. Hence, the key parameter for the MBH merger is the density of field stars in the regions where MBHs are distributed. The distance of an MBH binary at the pericenter shrinks through the sling-shot mechanism of another MBH. It is followed by the shrinking of the semimajor axis due to the energy loss by gravitational wave radiation, and eventually the binary merges. We have found that the secular angular momentum loss by the Kozai mechanism does not work for a binary to merge if the relativistic periastron shift is properly included. The present simulations imply that a large MBH can be formed from the system of multiple MBHs with smaller mass purely through N-body process. The present results are applicable for the different mass scales of a host galaxy and MBHs if the density of the host galaxy satisfies the scaling in the N-body units. This merger path can be important for the growth of MBHs in a primordial galaxy. Also, the MBH merger may be a potential source of gravitational waves for the *Laser Interferometer Space Antenna* (*LISA*) and pulsar timing.

We thank Toshiyuki Fukushige for helpful advice on the parallel N-body code, Takashi Okamoto for fruitful discussion on initial conditions, Masaki Iwasawa for useful comments about our simulation method, and the anonymous referee for meaningful advice on post-Newtonian approximation. Numerical simulations have been performed with computational facilities at the Center for Computational Sciences in the University of Tsukuba. This work was supported in part by the FIRST project based on the Grants-in-Aid for Specially Promoted Research by MEXT (16002003) and Grant-in-Aid for Scientific Research (S) by JSPS (20224002).

REFERENCES

Abel, T., Bryan, G. L., & Norman, M. L. 2000, ApJ, 540, 39
Abramowicz, M. A., Czerny, B., Lasota, J. P., & Szuszkiewicz, E. 1988, ApJ, 332, 646
Begelman, M. C., Blandford, R. D., & Rees, M. J. 1980, Nature, 287, 307
Berentzen, I., Preto, M., Berczik, P., Merritt, D., & Spurzem, R. 2009, ApJ, 695, 455
Blaes, O., Lee, M. H., & Socrates, A. 2002, ApJ, 578, 775
Boroson, T. A., & Lauer, T. R. 2009, Nature, 458, 53
Bromm, V., Coppi, P. S., & Larson, R. B. 2002, ApJ, 564, 23
Campanelli, M., Lousto, C., Zlochower, Y., & Merritt, D. 2007, ApJ, 659, 5
Damour, T., & Dervelle, N. 1981, Phys. Lett., 87, 81
Dotti, M., Montuori, C., Decarli, R., Volonteri, M., Colpi, M., & Haardt, F. 2009, MNRAS, 398, L73
Fabrycky, D., & Tremaine, S. 2007, ApJ, 669, 1298
Fan, X., et al. 2001, AJ, 122, 2833
Ferrarese, L., & Merritt, D. 2000, ApJ, 539, L9
Hernquist, L. 1990, ApJ, 356, 359
Iwasawa, M., Funato, Y., & Makino, J. 2006, ApJ, 651, 1059
Kesden, M., Sperhake, U., & Berti, E. 2010, ApJ, 715, 1006
Kormendy, J., & Richstone, D. 1995, ARA&A, 33, 581
Kozai, Y. 1962, AJ, 67, 591
Kupi, G., Amaro-Seoane, P., & Spurzem, R. 2006, MNRAS, 371, 45
Lousto, C. O., Campanelli, M., Yosef, Z., & Nakano, H. 2010, Class. Quantum Grav., 27, 114006
Magorrian, J., et al. 1998, AJ, 115, 2285
Makino, J., & Aarseth, S. 1992, PASJ, 44, 141
Makino, J., & Funato, Y. 2004, ApJ, 602, 93
Marconi, A., & Hunt, L. K. 2003, ApJ, 589, L21
McMillan, S. L. W. 1986, ApJ, 307, 126
Miller, M. C., & Hamilton, D. P. 2002, ApJ, 576, 894
Milosavljevic, M., Bromm, V., Couch, S. M., & Oh, S. P. 2009a, ApJ, 698, 766
Milosavljevic, M., Couch, S. M., & Bromm, V. 2009b, ApJ, 696, 146
Nakamura, F., & Umemura, M. 2001, ApJ, 548, 19
Ohsuga, K., Mori, M., Nakamoto, T., & Mineshige, S. 2005, ApJ, 628, 368
Soffel, M. H. 1989, Relativity in Astrometry, Celestial Mechanics, and Geodesy (Berlin: Springer)
Soltan, A. 1982, MNRAS, 200, 155
Sudou, H., Iguchi, S., Murata, Y., & Taniguchi, Y. 2003, Science, 300, 1263
Tremaine, S., et al. 2002, ApJ, 574, 740
Umemura, M., Susa, H., Suwa, T., & Sato, D. 2008, in AIP Conf. Ser. 990, First Stars III: First Stars III Conference, ed. B. W. O'Shea, A. Heger, & T. Abel (Melville, NY: AIP), 386
Yoshida, N., Omukai, K., Hernquist, L., & Abel, T. 2006, ApJ, 652, 6
Yu, Q., & Tremaine, S. 2002, MNRAS, 335, 965